

# **BONDING OF CFRP PRIMARY AEROSPACE STRUCTURES – CRACKSTOPPING IN COMPOSITE BONDED JOINTS UNDER FATIGUE**

T. Kruse<sup>1</sup>, Dr. T. Körwien<sup>2</sup>, S. Heckner<sup>3</sup> and Dr. M. Geistbeck<sup>4</sup>

<sup>1</sup> Airframe Research & Technology, Airbus Operations GmbH  
Kreetslag 10, 21129 Hamburg, Germany  
Email: [thomas.kruse@airbus.com](mailto:thomas.kruse@airbus.com), web page: <http://www.airbus.com>

<sup>2</sup>Material and Processes, Airbus Defence and Space GmbH  
Rechlinerstraße, 85077 Manching, Germany  
Email: [thomas.koerwien@airbus.com](mailto:thomas.koerwien@airbus.com), web page: <http://www.airbusdefenceandspace.com>

<sup>3</sup>Composites Technologies, Airbus Group Innovations  
Willy-Messerschmitt-Strasse, Ottobrunn, Germany  
Email: [sebastian.heckner@airbus.com](mailto:sebastian.heckner@airbus.com), web page: <http://www.airbusgroup.com>

<sup>4</sup> Composites Technologies, Airbus Group Innovations  
Willy-Messerschmitt-Strasse, Ottobrunn, Germany  
Email: [matthias.geistbeck@airbus.com](mailto:matthias.geistbeck@airbus.com), web page: <http://www.airbusgroup.com>

**Keywords:** composite bonding, fatigue, damage tolerance, crack stopping, aerospace, laser stripping, crack arresting, CLS

## **ABSTRACT**

Today the application of bonding technology for primary aerospace structures is limited due to the certification regulations. State of the art is the widely used chicken rivet which is limiting the benefits of the application of composite bonded joints.

This paper will give an overview on the actual research followed by the Airbus Group within the European project BOPACS. The Project is focussing directly on the application of Mean of Comply within AC-20-107B by investigating design feature as crack arrest features.

The central element for the characterisation of the crack arresting capability of different – features is the cracked lap shear (CLS) specimen. It represents realistic deformation behaviour of typical aircraft bonded joints and features constant tuneable mixed mode ratios over the full length.

The Study showed a reproducible crack initiation and repeatable crack growth and arresting characterizing the investigated feature alternatives as e.g. lockbolts, pins and surface modifications. Details on the results for different CLS-configurations to isolate the combined functionality of state of the art fasteners (e.g. bearing vs. clamping) will be discussed in details for pure tension fatigue tests. As the conventional CLS specimen shows a steady crack growth rate under tension, the crack growth in CLS samples under compression was investigated by analysis and test to determine if compression poses potentially more aggressive crack growth behaviour. For the latter, a test fixture was developed to compress buckling and to tweak the associated Mode I ratio. Test were performed with different set-ups.

As an alternative crack stopping concept a pulsed ultraviolet laser radiation was used to pretreat CFRP surfaces prior to the adhesive bonding process. In comparison to conventional surface preparation techniques higher bonding strengths and positive results concerning crack propagation were achieved.

## 1 INTRODUCTION AND STATE OF THE ART DESCRIPTION

With the entry into service of the A350XWB a consequent evolution of the usage of CFRP for primary structures within Airbus Group has reached the next milestone. After a long and excellent experience with CFRP in civil and military applications, first applied on secondary structures and since 1983 for the vertical stabilizer as first major primary structural component for civil aircrafts, Airbus Group has now reached the next step in the transition from a metallic to a composite aircraft with the first CFRP fuselage of an Airbus aircraft on A350 XWB.

One key technology for the future development of composite aircraft structures is a suitable joining technology. Mechanical fastening is still the state of the art joining method for primary airframe structures for metallic as also for composite structures. Bonding is one of the most promising alternative joining technologies especially for composite structures.

At the same time bonding is enabling new disruptive structural concepts based on new integration sequences, structure mechanic principles and joint geometries.

### 1.1 State of the Art Bonding Technology

#### 1.1.1 Classification of Bonding Technologies

Figure 1 shows the three main categories of joining of composites with thermoset matrices representing the different stages of integration.

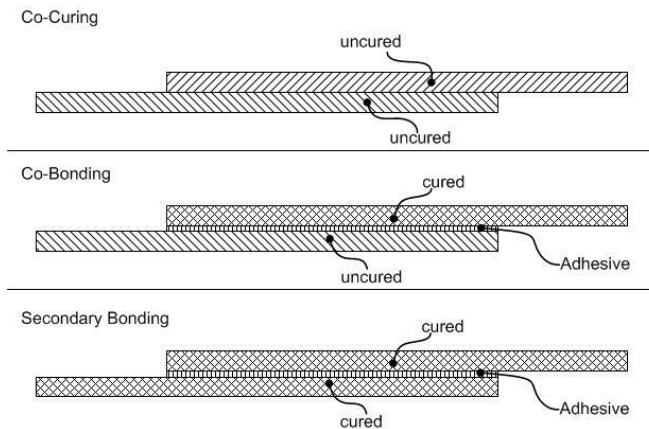


Figure 1: Classification of composite bonded joints

**Co-Curing** represents the earliest stage of integration, resulting in a fully integrated component. The joining mechanism is chemical cross-linking.

**Co-Bonding** represents an intermediate stage of integration. An uncured part is joined with one or more cured parts, typically with an additional layer of adhesive. The joining mechanism between the adhesive and the cured part is adhesion. Between the un-cured part and the adhesive chemical cross-linking is taking place.

**Secondary Bonding** represents the latest stage of integration. Two previously cured parts are joined by a film or paste adhesive. The joining mechanism between adhesive and adherend is adhesion.

#### 1.1.2 Definition of potential failure initiation modes

The following three failure initiation modes are describing the most important origins of potential failures of bonded joints. There are different root causes for these initial failure modes and only major effects will be discussed in this paper.

### 1.1.3 Disbond

A disbond is an initial area within a bonded joint without connection between adherend and adhesive. Typical root causes are massive contaminations of the adherend surface (e.g. with release agent) or failures within the adhesive application process (e.g. gaps within the adhesive layer). A disbond is detectable by means of nondestructive inspection technologies (NDI) as e.g. ultrasonic inspection within the individual limits of the detection threshold per technology.

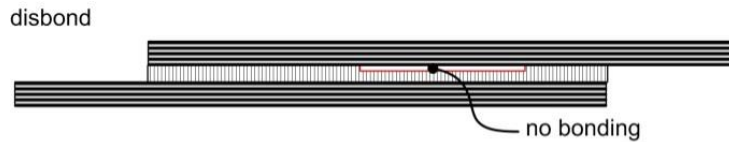


Figure 2: Failure initiation mode disbond

### 1.1.4 Weak bond

A weak bond is a bonded joint with reduced strength between adherend and adhesive. It is characterized by an adhesive failure mode. The root cause is an insufficient adhesion of the adherend interfaces due to small contamination of the surface or unfavourable process conditions.

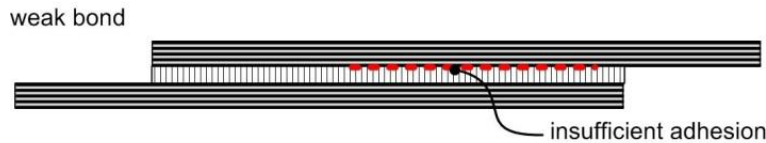


Figure 3: Failure initiation mode weak bond

A weak bond is not detectable by means of today's NDI methods due to the absence of a detectable interface layer. Research addresses the problem but results are not expected short- to mid-term for industrial usage.

### 1.1.5 Impact

Impact events within manufacturing and in service can lead to initial damages of the adherend and the adhesive. Damages resulting from impact are detectable by NDI within the individual limits of the detection threshold.

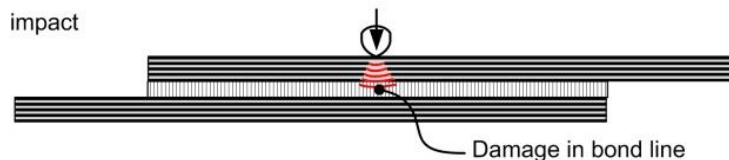


Figure 4. Failure initiation mode impact

## 2 CERTIFICATION COMPLIANCE

### 2.1 Bonded Aerospace structures within the context of certification boundary conditions

Resulting from the described State of the Art within the composite bonding technology today's certification rules according AC 20-107B [3] are limiting the certification of composite bonded joints to the following possible approaches:

*“For any bonded joint, the failure of which would result in catastrophic loss of the airplane, the limit load capacity must be substantiated by one of the following methods:*

- (i) *The maximum disbonds of each bonded joint consistent with the capability to withstand the loads in paragraph (a)(3) of this section must be determined by analysis, tests, or both. Disbonds of each bonded joint greater than this must be prevented by design features, or*
- (ii) *Proof testing must be conducted on each production article that will apply the critical limit design load to each critical bonded joint, or*
- (iii) *Repeatable and reliable non-destructive inspection techniques must be established that ensure the strength of each joint." [3]*

Today, no suitable NDI method to full fill the requirement [3]; (iii) of a secured measurement of the failure strength of a joint is in place. Moreover, it is not affordable to establish a full single part testing of each bonded joint within an industrial environment of a commercial aircraft manufacturing according to requirement [3]; (ii).

Therefore the only requirement [3]; (i) is practically to be taken into account for the sizing and certification of bonded joints.

State of the art to certify a structural composite joint is to follow approach [3]; (i) by the usage of additional fasteners which have to be capable to carry the relevant loads taking into account a global failure of the bondline. This boundary condition and the corresponding technical concept of additional fasteners are limiting the benefits of the application of composite bonded joints in terms of weight, cost and performance.

### **3 CRACKSTOPPING APPROACH**

#### **3.1 Context for certification**

To follow directly the directive provided by AC20-107B [3]; (i) the limitation of the maximum disbond to a non-critical size for each structural application is one feasible way within today's certification boundaries. The European funded Project BOPACS is focused on the development of crack stopping concepts to improve today's state of the art additional fasteners by two means:

First, by improved understanding of the crack stopping mechanism in composite bonded joints for primary structures with high and low load transfer configuration.

Second by development of novel crack stopping features as alternative to state of the art used fasteners.

#### **3.2 Validation approach**

Target within BOPACS is to demonstrate a secured crack stopping under fatigue in case of the presence of a local weak bond. For comparability all tests within BOPACS have been performed with full strength bonding and increased load level to exceed the stress level in the bondline above the no growth criterion for the healthy bondline.

The crack growth rate [mm/cycle] is representing the individual crack stopping capability of each tested configuration using the cracked lap shear (CLS) test as described in §4.1.

As the test is performed on an increased load level also slow growth behaviour can be accepted as for a realistic configuration and load spectrum an improved crack stopping performance can be expected.

The detailed no growth check with an assumed presence of a local weakbond has to be performed for each specific design solution.

### **4 EXPERIMENTAL INVESTIGATION**

#### **4.1 CLS test configuration**

For comparison of the different features and crack stopping configurations the cracked lap shear specimen (CLS) has been selected as this configuration represents best a typical ratio of mode I and mode II in combination with a realistic deformation constantly over a sufficient length of crack propagation.

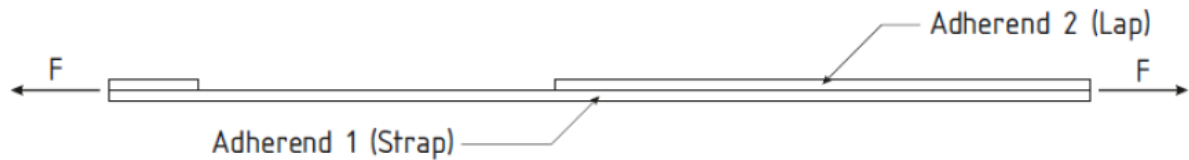


Figure 5: Principle Sketch of CLS Specimen

The Mixed Mode Ratio (MMR) differs only slightly in the relevant area of interest for crack propagation and the influence on the crack propagation rate has been proven as minor as shown in Figure 7.

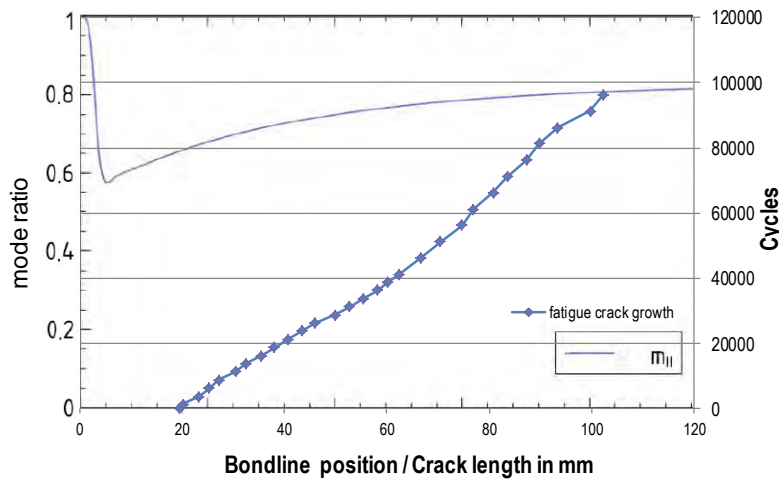


Figure 6: Mode ratio (FEA) vs. crack growth speed for CLS (Test)

All tests have been performed with quasi-isotropic laminates. The bonding has been performed with a combination of Henkel EA9395 with 20 % EA9396 paste adhesive after plasma treatment of the adherents.

#### 4.2 CLS Lockbolt parameter study

State of the art fasteners like lockbolts have been selected as baseline for benchmarking within BOPACS. Alternative features have to compete in terms of static strength of the bonding, crack stopping capability and also cost & lead time. Therefore, a good understanding of the different effects provided by a lockbold is mandatory for any benchmarking to be performed within BOPACS.

Also the lockbold offers the prerequisite to investigate and test separated effects like bearing, clamping force or diameter change in a simplified test setup.

Within this parameter set the following configurations have been tested:

- Reference without feature
- 4,8mm lockbolt
- 4,8mm lockbolt with axial clearance
- 4,8mm lockbolt with radial clearance (clearance fit)
- 4,0mm lockbolt
- 4,8mm open hole

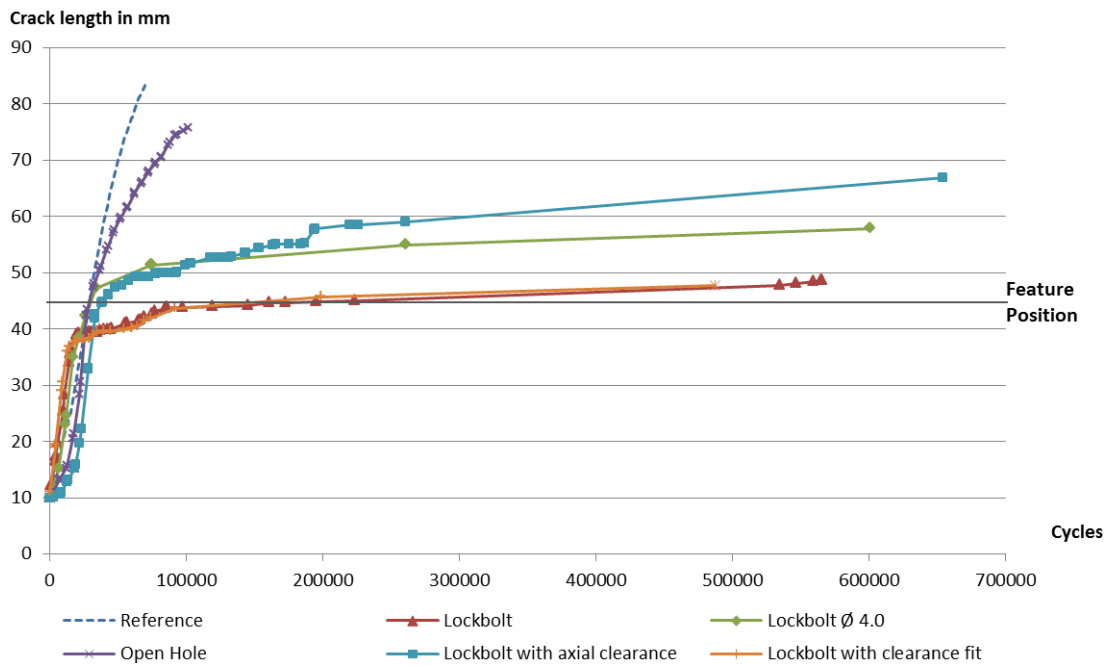


Figure 7: Comparison of investigated parameters

For all configurations with crack arresting capabilities the crack slows down behind the crack stopper position. The principle behaviour has been validated by FEM simulation as shown in Figure 8.

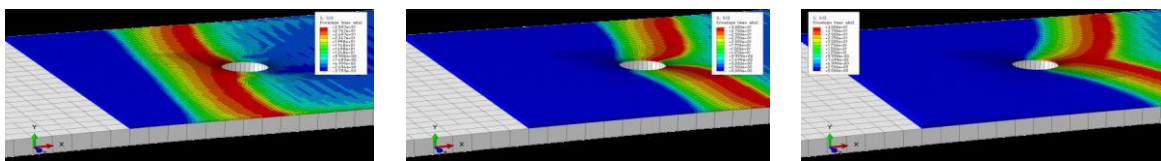


Figure 8: Pictures of FEM Simulations

### 4.3 Alternative crack stopping concept

One Stream of new crack stopping features within BOPACS is surface modification. The basic approach is to use adherent fibres as bondline reinforcement which will serve as crack stoppers, as depicted in Figure 9.

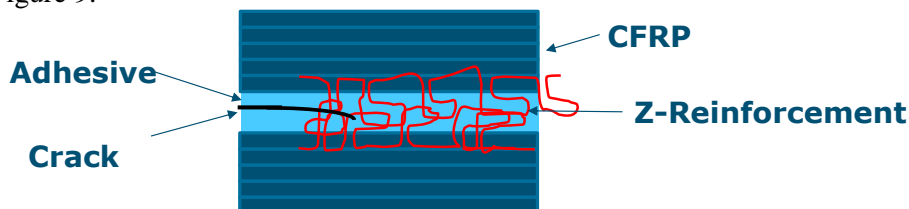


Figure 9: Principle of surface modification approach

For the implement of this approach, reinforcement in thickness direction of the bondline has to be created. Therefore, a modification of the top layer of the CFRP adherend is required. To get a multidimensional reinforcement in the adherend adhesive interface one option is to use a knitted fabric as a top layer within the CFRP lay-up. The surface fibers in the area of the bondline have to be exposed after manufacturing of the adherent.

### 4.3.1 Laser stripping trials

To expose the fibres in this investigation a laser ablation process was used. The laser source was a pulsed ns ultraviolet solid-state Q-switched laser with an average power of about 3W and a pulse duration below 20 ns.

By adapting scanning speed, hatch distance, repetition rate and focus size of the laser resin could be removed without fiber damage. The difference of the vaporization temperature for resin (427 °C) and carbon fibres (3727 °C) [1] is one enabler for the selective removal of resin.

Examples of laser treatment results on a unidirectional CFRP surface are shown in Fig. 10.

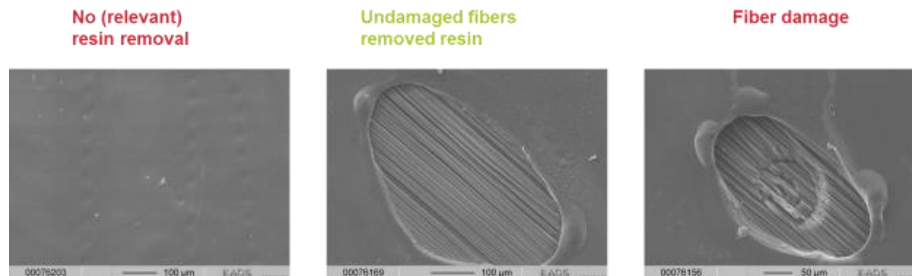


Figure 10: Comparison of the results between a low laser density (left), a optimized (middle) and a too high laser density (right)

### 4.3.2 Determination of adhesive strength by centrifugal pull off testing

To characterize the static strength of the bondline achievable on CFRP surfaces with laser exposed fibres a mechanical centrifugal test has been performed [2]. Untreated samples and samples treated with atmospheric plasma were used as reference.

The process parameters for the atmospheric plasma pretreatment were known from former investigations performed at Airbus Group Innovations. In all cases UD laminates were used as adherend materials.

Figure 11 shows that laser processed surfaces lead to high bond strength, which exceeds the strength achieved on CFRP surfaces treated by atmospheric plasma with optimized parameters for high adhesion strength.

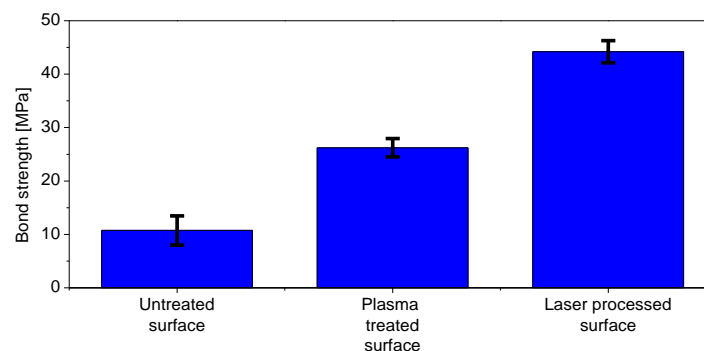


Figure 11: Bond strength on untreated, plasma treated and laser processed surface

### 4.3.3 Investigation of crack stopping performance

As a weakbond typically progresses at the interface between adherent and adhesive an initiation with the same failure mode has to be ensured for the testing. Experience from former projects allows the creation of weak bonds achieving defined bond strength by applying plasma treatment on the adherend surface with a specific set of plasma parameters.

Figure 12 shows the set-up for the CLS test. In this setup the strap surface in the bonded area had been treated with atmospheric plasma parameters yielding to an adhesive strength of 50%. The location of the crack stopping feature within the bondline is defined in Figure 12. The feature covers the full width of the CLS test sample.

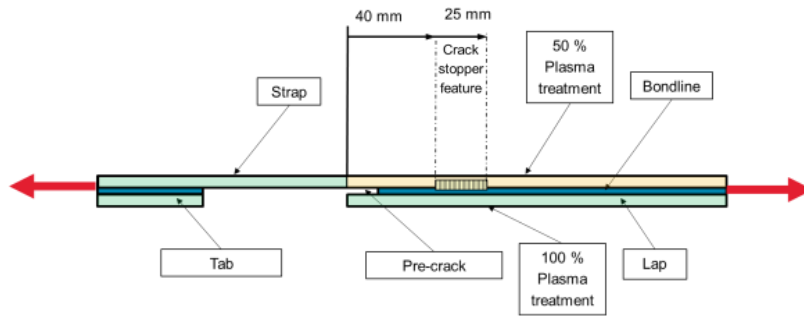


Figure 12: CLS Samples

The topography of the CFRP surfaces with exposed carbon fabric fibres after laser treatment is shown in the SEM picture of Figure 13. It could be proved that with laser parameters optimized on the UD CFRP surfaces it is possible to also expose the fibers on the surface of CFRP plate with a knitted fabric as top layer in the lay-up.

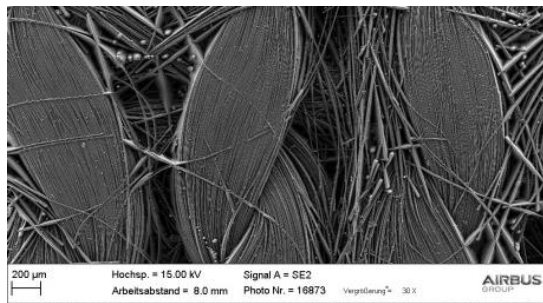


Figure 13: SEM picture of laser pretreated knitted fabric surface

The CLS tested sample in Figure 14 shows a pre-crack length of 20 mm for the left and 35,7 mm for the right side. The crack starts to grow quite fast from the beginning of the test at a load of 23,16 kN. After 10.000 cycles the crack length for the left and the right side are nearly the same with an average value of 40.9 mm. After reaching the crack stopping feature (indicated by the red lines in Figure 14) the crack speed is significantly slowed down.

At the initial load of 23,16 kN the crack length only slightly increases up to 41,9 mm at 600.000 cycles. Also with a stepwise increase of the load (25,47 kN after 600.000 cycles, 28,02 kN after 1.100.000 cycles, 30,83 kN after 1.600.000 cycles) the crack growth is very low. The crack has not exceeded the crack-stopper area within more than 2 million cycles, despite several load increases.

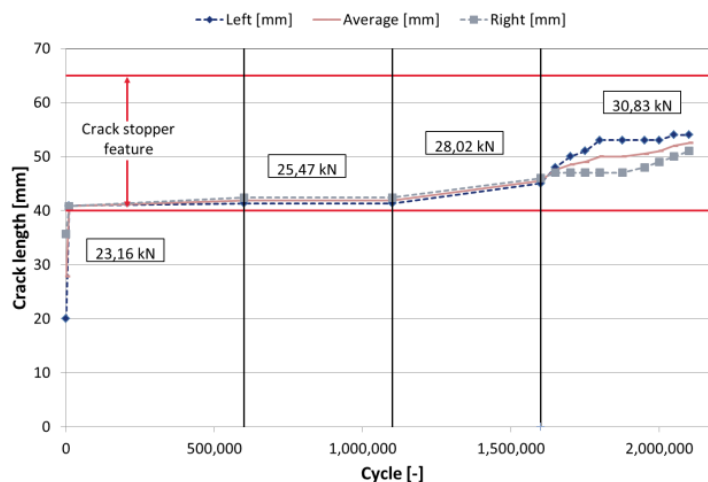


Figure 14: Second CLS test for a sample with a crack stopper feature



#### 4.4 Experimental CLS-compression

Specimens under tensile load exhibited a reliable crack growth behaviour. While under tension the lap bends away from the strap thus creating a mixed mode in dependency of the material properties. Under compression the lap tip pushes against the strap. Preliminary simulation suggested a bending of the strap that created a bridging effect thus leading to mode I in the bridging area, refer to Figure 15.

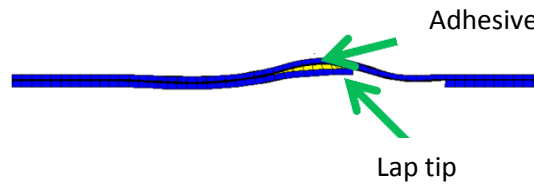


Figure 15: Bridging effect of the specimen

This section investigates the behaviour of the specimen under compression load. It will answer the question if a compression load will produce more aggressive crack growth behaviour under fatigue than tensile load.

##### 4.4.1 Development of a clamping fixture

The critical buckling force for the standard CLS-specimen has been determined with 20 kN. The tension fatigue test with CLS specimens in the BOPACS project were mainly conducted with 23,16 kN which according to calculations and the simulation is nearly the buckling load for compression. In order to protect the specimen against buckling a clamping device has been developed. The clamping device clamps the specimen with rolls. The rolls in the middle enable the tuning of the mode I ratio during test. Figure 16 shows a picture of the clamping device.

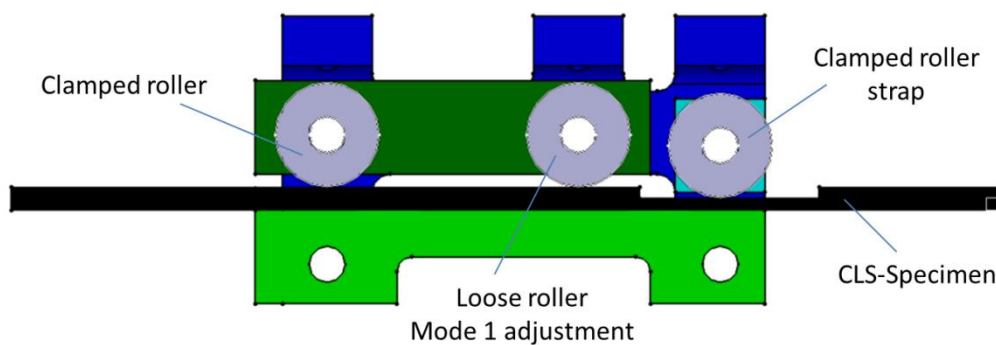


Figure 16: Modified clamping device with rolls

##### 4.4.2 Static compression test with clamping device

First a static test has been performed in order to evaluate the strain levels for certain loads to compare the tests with simulations. Furthermore, it was to check if and how the specimen bends. The specimen was clamped on the outer four rolls of the clamping device.

The result of this approach was that the strain levels linear even up to high loads. The offset of strain gauge A to strain gauge C is reflecting the bending. Therefore, it was expected to have an increased Mode I loading that leads to crack propagation during the fatigue test.

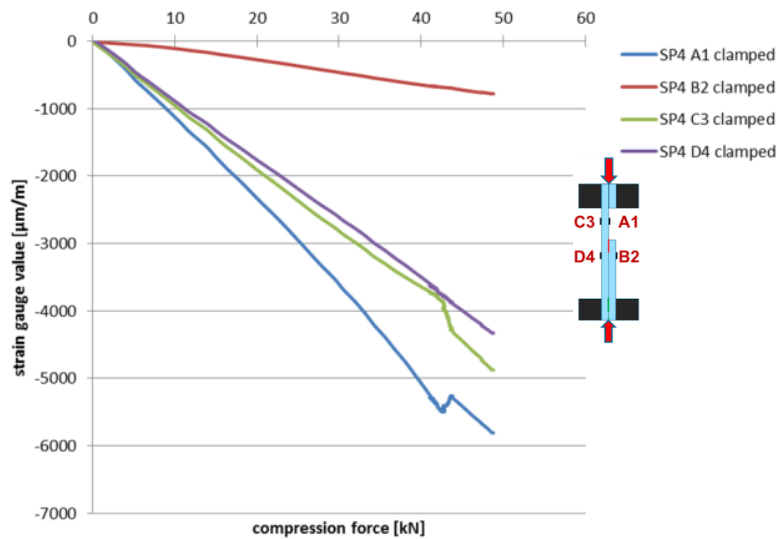


Figure 17: static compression test

#### 4.4.3 Fatigue compression tests

The setup of the specimen and the clamping device reflects the static test setup. The aim of this test is to find a load level which leads to crack propagation. The initial load level of the fatigue test has been defined at 17,5 kN with 8 Hz and checked after 30.000 cycles for crack propagation. If not observed the load would be raised by 2.5 kN for additional 30.000 cycles. The crack propagation has been measured with an ultrasonic A-scan. If a crack appears the current load level would have been maintained.

In the selected test setup up no crackgrowth has been observed up to 30 kN final load and in total 180,000 cycles. 30 kN already leads to critical strain levels in the specimen (stability / strength), no further increase has been applied.

Subsequently, the clamping device has been removed and 30,000 cycles with 15 kN compression load without crack growth have been applied. Figure 18 shows, as an example, the related results of the test.

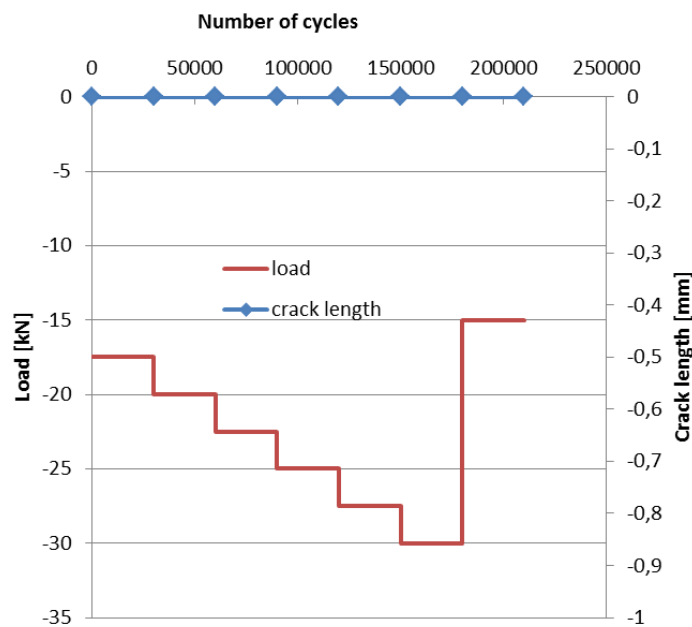


Figure 18: compression fatigue test

#### 4.4.4 Fatigue compression tests with elongated initial crack

After the first trial did not lead to crack propagation at different compression load levels a new approach was followed to foster a fatigue cracking under compressive load. The approach was to elongate the initial crack, thus enlarging the bridging area. So the strap bending due to the compression load would lead to mode I in the bondline vicinity. The crack elongation was achieved by fatigue tension loading. From previous tension fatigue tests with 23.16 kN the resulting crack propagation for a certain cycle number can be very exactly predicted. To be sure about the new initial crack length, the crack frontline was detected with US-A-scans. In a first step the crack has been elongated to a total initial crack length of 32 mm within 30,000 cycles. Subsequently a fatigue compression test with a load of 23.16 kN has been conducted.

Testing with additional 30,000 cycles compression load did not lead to any further crack propagation. Also 30,000 cycles compression fatigue testing after further increase of the pre-crack to 43 mm and 51 mm and subsequent additional 200,000 cycles has shown no crack propagation.

With a total of 550,000 cycles for several compression and tension load levels only crack propagation in the adhesive could be observed for tension load (50,000 cycles). The 500,000 cycles compression load did not lead to a fracture of the adhesive. Figure 19 summarizes the test results. As main effect leading to this no-growth behaviour under compressive loading the local suppression of Mode I at the crack tip has been identified.

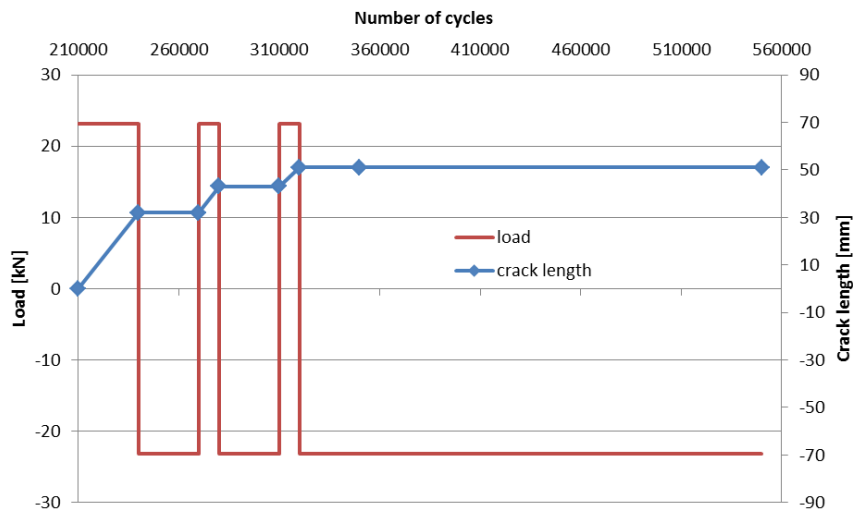


Figure 19: Specimen No. 5 fatigue test row 3

Figure 20 shows the specimen after the test. The white lines display the crack frontline at the different applied tension fatigue cycles (crack growth from left to right).



Figure 20: Crack propagation for tension load

## CONCLUSIONS

Certification of structural bonded joints requires compliance to at least one out of three means. The limitation of crack growth below a critical limit is the most feasible and practised approach. BOPACS investigates the principles of crack growth in bonded joints. The tested CLS configurations showed

steady and reproducible crack growth behaviour.

A parametric study has been performed using lockbolts as crack stopping elements. These elements proved suitable to significantly slowing of the crack progression in any configuration tested. Also a better understanding of the isolated parameters could be gained.

To eliminate lockbolts as crack stopping element alternatives have been investigated. Laminates with a surface layer of knitted fabric were stripped using laser in order to free up fibers. These fibers were intended as bondline reinforcement for crack stopping. The tested configurations showed good crack arrest capabilities even under increased load level. All tests were carried out under tension, though. In order to prove that tensile load is the critical load case for CLS, a side study was carried out to investigate the compression behaviour of CLS Specimen under fatigue. In all the investigated CLS compression tests no crack growth has been observed, even without buckling fixture.

### ACKNOWLEDGEMENTS

This work has been carried out within the framework of BOPACS as funded activity by the European Commission within the FP7 Framework. The authors would like to thank the BOPACS consortium for their support. Most of the tests were professionally carried out at VZLU in Prague and IFAM in Bremen. Furthermore the authors want to thank the following Students for contribution within their Thesis to the results presented in this paper: Arnd Köppe, Katharina Hoidis, Tobias Mayr, Phillip M. Huber.

### REFERENCES

- [1] R. Negarestani, L. Li, H.K. Sezer , D. Whitehead, J. Methven, Nano-second pulsed DPSS Nd:YAG laser cutting of CFRP composites with mixed reactive and inert gases, *The International Journal of Advanced Manufacturing Technology*, 49 (5-8), 2010, pp. 553–566.
- [2] T. Koerwien, *FFS - Statistische Ansätze zur Verbesserung der Zuverlässigkeit geklebter CFK Verbindungen*, Deutscher Luft- und Raumfahrtkongress, DGLR, Augsburg, 2014.
- [3] U.S. Department of Transportation - Federal Aviation Administration (FAA), *Advisory Circular - Composite Aircraft Structure*, AC-107B, FAA, 2009.
- [4] J. Halm et al., *Part B - Project Proposal: Boltless assembling of primary aerospace composite structures*, BOPACS, 7<sup>th</sup> Framework Programme for EU R&T, Amsterdam, 2011